

Evaluation of a Fully-Integrated Cardiac SPECT/VCT System Using a Common Set of Solid-State Detectors for Both Emission and Transmission Scans and a Novel Low Dose Lead Fluorescence X-ray Transmission Line Source

Chuanyong Bai, *Senior Member, IEEE*, Hetal Babla, *Member, IEEE*, Joel Kindem, Richard Conwell, *Member, IEEE*, Randy Weatherhead

Abstract-- We developed a new rapid imaging cardiac SPECT system (Cardius® X-ACT) with a low dose volume CT transmission-based attenuation correction (AC). Three solid-state detectors are configured to form a triple-head system for emission scans and reconfigured to form a large 27" (69 cm) field-of-view detector arc for transmission scans. The near mono-energetic transmission line source is the collimated fluorescence X-ray emitted from a lead target when the lead target is fluxed by a narrow X-ray beam from an X-ray tube. When the X-ray tube operates at 160 kVp and 2.0 mA, the line source has a flux density of 80 times that of conventional isotopic sources. High quality transmission scans can hence be completed in as short as one minute with insignificant patient dose (~5 μ Sv). For evaluation, we scanned an anthropomorphic phantom with a uniform cardiac insert and the same anthropomorphic phantom with one 60° full defect and one 45° 50% defect in the cardiac insert. We also scanned an ACR phantom and a uniform cylindrical phantom (with water). Results showed that image uniformity and defect contrast were improved by AC in the anthropomorphic phantom studies as compared to without AC (NAC). The 17-segment scores of the images of the uniform cardiac insert were 78 ± 6 before and 88 ± 3 after AC (average \pm standard deviation). The inferior to anterior wall ratio and the septal to lateral wall ratio were 0.99 and 1.16 before and 1.02 and 1.00 after AC. The defect contrast of the full and 50% defect was 0.528 and 0.156 before and 0.628 and 0.173 after AC. The ACR phantom images with AC showed correction of the bowing effect due to attenuation in the NAC images. The reconstructed attenuation coefficient of water at 140 keV was $0.151 \pm 0.003/\text{cm}$ and $0.151 \pm 0.002/\text{cm}$ in the liver and cardiac regions of the anthropomorphic phantom, and $0.150 \pm 0.003/\text{cm}$ in the uniform region of the ACR phantom and the uniform cylindrical phantom. In conclusion, the X-ACT system generated accurate attenuation maps with one-minute transmission scans. Phantom studies showed that AC improved image quality and quantification over NAC.

Key words: Attenuation Correction, Cardiac SPECT, Solid-State Detector, Fluorescence X-ray Transmission Source

I. INTRODUCTION

In myocardial perfusion cardiac SPECT imaging, non-uniform attenuation is generally recognized to be the most important contributor to the diagnostic inaccuracy [1]. Non-uniform attenuation can alter the absolute and relative pharmaceutical uptake and introduce artifacts into the images. Such artifacts, when not identified, may be incorrectly interpreted and could lead to inaccurate diagnostic results. In practice, experienced nuclear cardiologists can use some complimentary techniques such as dual stress and rest scans, ECG gating and combined supine/prone or

upright/semi-recumbent imaging to read around the attenuation artifacts [2]. However, attenuation correction (AC) that directly corrects the attenuation artifacts is believed to be a more scientific way [3] to increase the diagnostic accuracy of myocardium perfusion SPECT imaging.

Mounting evidences demonstrate that when AC is performed appropriately, it improves the accuracy of myocardium perfusion SPECT as the theory of AC predicts and may also improve laboratory efficiency as compared to the complementary techniques, such as using a stress only protocol with AC for selected patients instead of the dual stress/rest scan protocol [4]. A collection of references to these evidences can be found in [5]. For the future of myocardium perfusion SPECT, the role of AC is even more critical. As pointed out by Watson [6], AC could not only make image interpretation easier, but could also open the door to a new level of diagnostic capability through the imaging of the true quantification of tracer uptake of which AC is a prerequisite.

The American Society of Nuclear Cardiology (ASNC) and the Society of Nuclear Medicine (SNM) issued a joint position statement [5] that "incorporation of AC in addition to ECG gating with SPECT myocardial perfusion images will improve image quality, interpretive certainty, and diagnostic accuracy." The ultimate goal of AC is to improve the effectiveness of care and to reduce health care costs. For this very reason, a successful design of an AC system should on the one hand make AC accurate and on the other hand try to keep the cost of AC low.

In order to make accurate AC possible, a SPECT system with AC should meet the basic AC-related requirements, in addition to the emission imaging-related ones. These include, but are not limited to,

- (a) Capability of generating high quality attenuation images for accurate AC: accurate, low noise, no respiratory motion artifacts, no critical truncation [1, 6];
- (b) Low percentage of studies requiring manual transmission/emission registration [6]; And
- (c) Advanced reconstruction algorithms that incorporate non-uniform AC, non-stationary detector response correction, photon scatter,

and others if identified as critical to the accuracy of AC [1, 5].

To keep the AC cost low, a system should have

- (a) Low initial system cost, low siting expenses (lead-lined shielding, more power, or larger space), and low maintenance cost;
- (b) Low operational cost that can be achieved by reliable and fast transmission scans (as short as one minute); And
- (c) Low transmission dose to both patients and operators. If the dose is high, operational cost may be substantially increased because some states require additional personnel (other than a single Nuclear Medicine technologist) or a Nuclear Medicine technologist with special certification to perform the transmission scans.

Conventional isotopic AC systems use the same Anger detectors to acquire both the emission and transmission data with isotopic transmission sources in the form of point, line, or an array of point or line sources. Isotopic transmission sources used in cardiac SPECT have strength limitations (usually less than 1 Ci) because of availability, cost, and handling considerations. Also, due to the relatively low count rate capacity of Anger detectors, the transmission source strength must be limited even if ultra strong transmission sources are available. The combination of these two facts leads to relatively low transmission flux rate that eventually lengthens the transmission scan times (e.g. 3 minutes or longer) and limits the quality and quantification accuracy of the obtained attenuation maps. Considering that the time required for emission scans can be as short as 3-4 minutes on state-of-the-art cardiac SPECT cameras today that use rapid imaging geometry in combination with advanced 3D reconstruction [7], the need to reduce the long transmission time inherent with isotopic approaches is critical. Furthermore, the transmission acquisition time has to be adjusted (lengthened) to compensate for the flux rate decrease as the isotopic sources decay. The sources have to be replaced at regular intervals to maintain the performance of the system, substantially increasing the operational cost of the system.

Newly developed in-line hybrid SPECT/CT systems convert the CT images to attenuation maps for SPECT AC [8]. The attenuation maps are virtually noise-free as compared to those from the isotopic AC approaches. However, current methods have demonstrated a high percentage of misregistration of the transmission and emission images. For example, Goetze and Wahl reported that misalignment may occur in up to 42% of the cases [9]. A major reason of the high percentage of misregistration is that CT scans are much faster than SPECT scans so that the two may capture

different patient respiratory motion patterns. Additionally, converting CT images to attenuation maps for attenuation correction at the emission energy is complicated and needs careful calibration for different operation X-ray kVp's [10]. Other factors that degrade the quality of the attenuation map converted from the CT images include the beam hardening effects in CT images and image truncation due to the relatively small CT field-of-view (FOV) [3].

Cost wise, in-line hybrid SPECT/CT systems require a separate CT detector system and a dedicated X-ray tube, greatly increasing the overall cost of the system. The CT systems used in these in-line designs may be diagnostic or non-diagnostic and range from single slice to 64 slices. The in-line SPECT/CT systems generally require very large rooms, high power and extensive site renovations (such as lead-lined shielding). The associated cost can easily exceed the cost of the SPECT system itself. From the patient dose perspective, the dose introduced by CT scans can be 100 to 1000 times higher than isotopic approaches. In a number of states, the higher dose of diagnostic quality CT systems may require an X-ray or CT technologist to perform the CT scans, significantly increasing the operational cost and increasing workflow complexity.

Recently, Digirad Corporation (Digirad, Poway, CA, USA) developed a novel, fully-integrated, rapid cardiac SPECT/Volume CT (VCT) imaging system (X-ACT) with AC capability [11]. It features proprietary high count rate capable solid-state detectors that are used for both emission and transmission scans. The use of these detectors in combination with a novel lead fluorescence X-ray transmission source enables high quality transmission scans to be completed in as short as one minute and emission scans in as short as three minutes. The accuracy, speed, and low associated cost of AC using the X-ACT system make it an ideal system for dedicated cardiac SPECT imaging with attenuation correction.

In this work, we first describe the basic configuration and specifications of the X-ACT system for cardiac SPECT imaging, then use phantom studies to evaluate its performance for attenuation correction. Finally, we discuss some of the practical advantages of using the X-ACT system for cardiac SPECT attenuation correction in routine clinical applications.

II. METHODS

A. System Configuration

The X-ACT system consists of three 20 cm x 15 cm detector heads. Image acquisition uses an upright geometry, where the patient sits in a chair that rotates during the data acquisition while the detector heads stay

stationary. Each detector is mounted with a high sensitivity fan-beam collimator. The detector heads are solid state and can operate at counting rates in excess of 5M cps per 20 cm x 15 cm detector area.

1) Emission Mode

In the emission mode the detectors are oriented to point at the axis-of-rotation (AOR) of the system. During setup, the patient's heart is positioned on the AOR by translating the chair (cardio-centric imaging, Fig. 1). As a result of this setup, the patient's heart remains in the center of the emission imaging field-of-view throughout the emission scan. This high-efficiency triple-head configuration [12] used in combination with 3D-OSEM reconstruction enables emission scans to be performed up to four times faster than that of a conventional dual-head system [7]. SPECT emission studies can be completed in as little as 3 minutes.

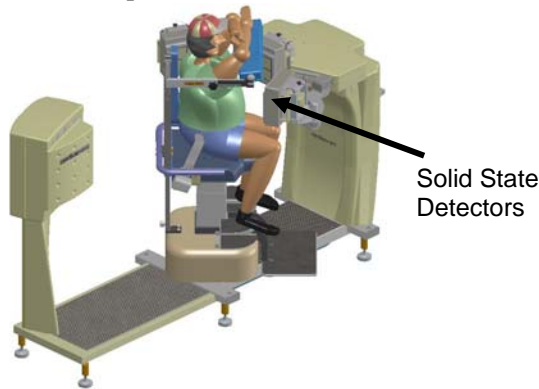


Fig 1. X-ACT system Configuration for emission scans.

2) Transmission Mode

When the emission acquisition is completed, the patient and chair stay stationary. The three detectors automatically reconfigure to form a single large 27" (69 cm) FOV detector arc (Fig. 2). The focal line of the collimator of each head co-aligns with the spatial location of the transmission line source to form a fan-beam transmission acquisition geometry. The effective transmission imaging FOV is 50.0 cm with the detector arc 39.1 cm away from the AOR. Since the patient's heart stays at the AOR of the transmission scan as well, the 50-cm FOV essentially makes the critical left side truncation of the patient [13] impossible, demonstrating a significant advantage of the X-ACT system over other hybrid SPECT/CT systems or small FOV SPECT systems using isotopic transmission sources for cardiac SPECT. For very large patients, transmission truncation using the X-ACT system can only occur at the right side of the patient. Since the right side truncation is non-critical for accurate AC, truncation compensation is not necessary for attenuation correction using X-ACT.

3) Transmission Line Source Assembly

The transmission source assembly [14] on the X-ACT system consists of a lead target, a low-dose X-ray tube, a lead collimator, and lead shields. When a transmission scan is started, the X-ray tube is turned on, and a narrow X-ray beam from the tube illuminates the lead target. The lead target in turn emits lead fluorescence X-ray photons. The lead target is positioned at the focal line of the fan-beam transmission acquisition geometry. The lead collimator collimates the lead fluorescence X-ray photons in both axial and transaxial directions to form the effective transmission line source [Fig. 3(a)]. The assembly is designed so that the X-ray beam from the X-ray tube does not exit the collimator directly. The transmission flux rate of the X-ACT system, when the X-ray tube is operated at 160 kVp and 2.0 mA, is about 2080 counts per pixel per second. Compared to about 500 counts per pixel per 20 seconds (25 counts per pixel per second) in conventional SPECT systems with isotopic transmission sources [15], X-ACT transmission source shows a factor of over 80 times increase in the flux density. Note that this comparison uses the same pixel size of 3.5 mm.

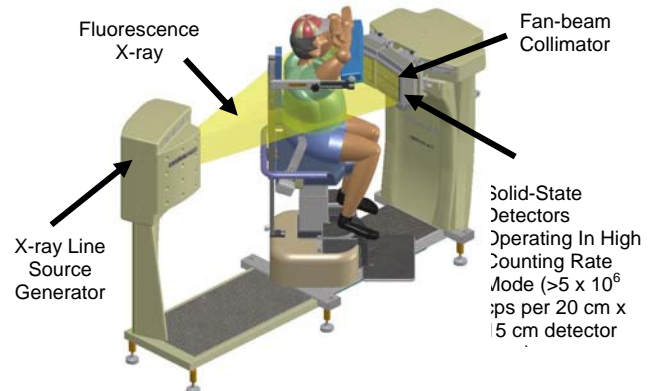


Fig 2. X-ACT system Configuration for transmission scans.

The lead fluorescence X-ray energies at different emission lines and their relative intensities [16] are shown in Table 1. The energies of the five emission lines are confined in a narrow range from about 73 to 87 keV. The generated transmission source of the X-ACT system is virtually a monoenergetic source centered at 77 keV [Figure 3(b)] as seen by the detectors, leading to no beam hardening artifacts for the intended use.

4) Image Reconstruction

For transmission image reconstruction, the transmission data is first corrected using the acquired emission contamination data. The logarithm of the ratio of the reference (from blank scan) to the transmission data is then calculated for each pixel to obtain the line integral of the linear attenuation along the corresponding line. Finally, a two-dimensional OSEM algorithm is used to reconstruct the attenuation map.

After the reconstruction, the value of each voxel of the attenuation map is scaled as follows:

$$mI = \frac{mu \times 1000}{\mu 77 \times pxlsz}, \quad (1)$$

where mu is the reconstructed value in the voxel, $\mu 77$ is the linear attenuation coefficient of water at 77 keV, $pxlsz$ is the pixel size of the map, and mI is the short integer after scaling. After this scaling, the attenuation map is essentially a low-resolution volume CT image (with voxel value equal to the corresponding Hounsfield unit plus 1000). The scaling is done for the purposes of image storage, communication, and display only.

Table 1. Energies and relative intensities of the five lead (82Pb) X-ray emission lines (100 is assigned to the strongest line) [16].

	$K\alpha_2$	$K\alpha_1$	$K\beta_3$	$K\beta_1$	$K\beta_2$
E(keV)	72.8	75.0	84.5	84.9	87.3
Intensity	60	100	12	23	8

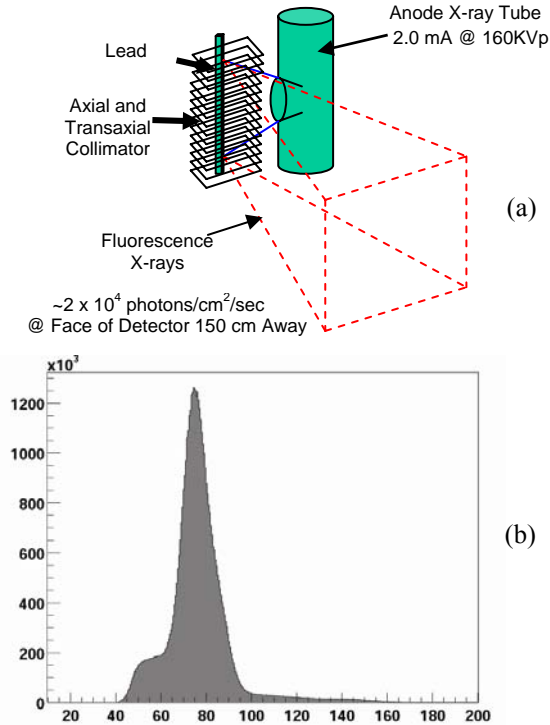


Fig. 3. (a) Illustration of transmission line source generation. The red dash lines depict the transmission flux. (b) The transmission flux spectrum measured on the X-ACT system that peaks at 77 keV.

For emission image reconstruction, X-ACT uses a 3D-OSEM algorithm that models depth-dependent spatial resolution, non-uniform attenuation [17], and photon scatter [18]. When used for AC, the saved attenuation map is scaled voxel by voxel to give the linear attenuation value for each voxel at the energy of interest. For example, for Tc-99m,

$$mu = \frac{mI * pxlsz \times \mu 140}{1000}, \quad (2)$$

where $\mu 140$ is the linear attenuation coefficient of water at 140 keV.

5) Other Aspects

Our previous work showed that the X-ACT system transmission scans included enough number of respiratory cycles such that the transmission images had essentially the same average effect of the respiratory motion as in the emission scans [19]. Patient studies in [20] showed no respiratory motion introduced aliasing artifacts in the transmission images. Transmission emission misregistration occurred in 20% of the cases, demonstrating a significant reduction as compared to the 42% that was reported of the hybrid SPECT/CT system in [9]. Preliminary clinical studies of low-likelihood patients using quantitative analysis [21] showed that AC significantly improved the myocardium uniformity versus NAC.

B. Uniform Cylindrical Water phantom Study

For phantom evaluation, we first performed the SPECT/TCT protocol 1 per the ASNC guidelines [22]. A cylindrical phantom with diameter of 20 cm and height of 20 cm was filled with water, followed by introduction of 5.0 mCi (185 MBq) Tc-99m activity. Emission scan was performed in a step-and-shoot mode with 10 seconds per step for a total of 20 steps. The resulted emission data thus had 60 projection views in 202.5° due to the triple-head acquisition. Transmission scan was performed in a continuous mode with the heads stationary and the chair rotated 206° in 33 seconds followed by the emission contamination scan in the same angular range but the reversed direction. The total acquisition time for transmission scan was thus 66 seconds. The radius of the circular orbit of acquisition was 21.0 cm.

The ASNC guidelines require that the reconstructed attenuation coefficient of water at 140 keV should be in the range of 0.145 - 0.161 cm^{-1} . The AC image should be more uniform than the NAC image.

C. Anthropomorphic Phantom Study with Uniform Cardiac Insert

Following the SPECT/TCT protocol 2 per ASNC guideline [22], we performed an anthropomorphic torso phantom (38 cm x 26 cm, Data Spectrum Corporation, Hillsborough, NC, USA) study with uniform cardiac insert. The recommended Tc-99m activity introduction to the phantom is with following concentration:

Heart:	6.8 μ Ci/cc (252 kBq/mL)
Background:	0.7 μ Ci/cc (26 kBq/mL)
Liver:	4.0 μ Ci/cc (148 kBq/mL)
Lungs:	0.0 μ Ci/cc (0 kBq/mL)

The phantom was placed on the patient chair with its cardiac insert positioned at the AOR by translating

the chair. The emission scan was acquired with 30 second per step with a total of 20 steps. Again, the emission data had 60 projection views in 202.5°. The transmission data was acquired with one minute followed by another minute of the acquisition of emission contamination data. The radius of the circular orbit of acquisition was 25.4 cm.

The ASNC guidelines require that the reconstructed attenuation coefficient of water at 140 keV should be in the range of 0.145 - 0.161 cm⁻¹ measured in two small regions of interest (ROIs), one at the liver and one at the cardiac insert. The AC image should be more uniform than the NAC image and no region of the heart in the AC images should be noticeably hotter than the rest. The anterior-posterior and septal-lateral ration should be in the range of 1.0±0.1.

We performed visual assessment of the uniformity of the AC and NAC images based on 3-view images. For quantitative assessment, we first did the ASNC specified wall ratio calculation then a 17-segment perfusion score statistic test as another level of uniformity analysis. For the statistic test, we first generated the 17-segment perfusion scores using QPS (Artificial Intelligence in Medicine, Cedars-Sinai Medical Center, CA, USA) and then calculated the mean and standard deviation of the segment scores. Since the segment scores are normalized to the maximum voxel value on the myocardium wall and the maximum voxel value is set to 100 in QPS, a more uniform image should have an average segment score closer to 100 and a smaller standard deviation than a less uniform image. When using QPS, wall scores for the wall ratio test were obtained using QPS → results → Grid → Walls option. For this analysis, the whole polar map is divided into five segments, including the central circular segment as apex and the other four as anterior, lateral, inferior, and septal walls. The 17-segment perfusion scores were obtained using QPS → results → Grid → Segments. Sample results of the 17-segment score maps are shown in the results section.

D. Anthropomorphic Phantom Study with Non-Uniform Cardiac Insert

Using the same anthropomorphic phantom and acquisition protocol above (Section II C) but with two defects in the cardiac insert, we tried to evaluate the effect of AC on the defect contrast (DC) in the reconstructed images. One defect was a 60° full defect located at the mid-anterior wall and the other was a 45° 50% defect located at the basal-inferior wall. The radius of the circular orbit of acquisition was 25.8 cm.

After image reconstruction, we first generated the 17-segment perfusion scores of the image of the cardiac insert, then calculated the defect contrast for each defect as

$$DC = \frac{Bkg - Def}{(Bkg + Def) / 2.0}, \quad (3)$$

where *Def* is the perfusion score of the segment with the defect and *Bkg* is the average of the perfusion scores of the direct neighboring segments of the segment with the defect. This calculation was done for both the AC and NAC images for comparison.

E. ACR Phantom Study

Finally, we performed an ACR phantom (Deluxe Jaszczak Phantom, Data Spectrum Corporation, Hillsborough, NC, USA) study per the American College of Radiology procedure [23]. The phantom was filled with 15 mCi (555 MBq) of Tc-99m. The emission data was acquired with 20 second per step and a total of 20 steps. The acquired emission data had 60 projection views in 202.5° with a total of 28 million counts. The radius of the circular orbit of acquisition was 21.0 cm.

For all of these phantom studies, the X-ray tube was operated at 160 kVp and 2.0 mA. The fan-beam collimator had a focal-length of 150.0 cm, hole size of 0.15 cm, and thickness of 2.7 cm.

III. RESULTS

A. Accuracy of the Reconstructed Attenuation Maps

Fig. 4 shows a transaxial slice of the uniform cylindrical phantom, two slices of the anthropomorphic phantom, one at the cardiac insert region and one at the liver region, in the reconstructed attenuation maps of the phantoms. White circles in the images show the ROIs used for quantitative analysis of the maps.

The detailed ROI information and the quantitative results of the mean and standard deviation are stated below. The reconstructed attenuation maps are quantitatively accurate according to the ASNC guideline requirement and of very low noise.

- Cylindrical phantom: slice thickness: 0.65 cm, ROI radius: 9.49 cm, number of voxels in ROI: 667, the reconstructed attenuation coefficient of water @140 keV in the ROI: 0.150±0.003 cm⁻¹ (mean ± standard deviation). The results for the uniform area of the ACR phantom were the same. Note that ASNC guidelines require the summation of multiple reconstructed slices to form a 5-cm slice for quantitation. We used only one reconstructed slice (slice thickness of 0.65 cm) because the image was

uniform enough and did not need the average over multiple slices for better quantitation.

- Anthropomorphic phantom, heart region: slice thickness: 0.65 cm, ROI radius: 5.33 cm, number of voxels in ROI: 213, the reconstructed attenuation coefficient of water @140 keV in the ROI: $0.157 \pm 0.006 \text{ cm}^{-1}$ (mean \pm standard deviation). Note that the ROI for attenuation coefficient calculation for the heart region included the Lucite “membrane” of the cardiac insert (the solid thin layers of material that defines the “left ventricle wall” of the insert), which has a density of 1.19 g/cc (19% higher than that of water, i.e., 1.0 g/cc). When the cardiac insert was moved out and the scan was repeated, the attenuation coefficient of water at the same ROI was $0.151 \pm 0.002 \text{ cm}^{-1}$.
- Anthropomorphic phantom, liver region: slice thickness: 1.95 cm, ROI radius: 6.37 cm, number of voxels in ROI: 304, the reconstructed attenuation coefficient of water @140 keV in the ROI: $0.154 \pm 0.004 \text{ cm}^{-1}$ (mean \pm standard deviation). When a smaller ROI (radius 3.51 cm, 88 voxels) was used so that the ROI did not touch the liver boundary (also made of Lucite), the mean \pm standard deviation was $0.151 \pm 0.003 \text{ cm}^{-1}$.

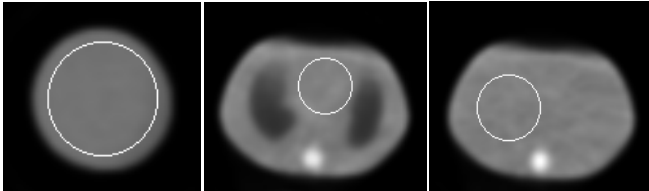


Fig 4. Reconstructed attenuation maps of the uniform cylindrical phantom and the anthropomorphic phantom. The white circles are the ROIs used for the attenuation coefficient calculation.

B. Image Uniformity

Fig. 5 shows the images of the uniform cardiac insert of the anthropomorphic phantom and the 17-segment perfusion maps and scores. Table 2 illustrates the quantitative results, including inferior to anterior wall ratio (Inf/Ant), septal to lateral wall ratio (Sept/Lat), and 17-segment perfusion scores (average \pm standard deviation). AC significantly improved the uniformity of the image, both visually and quantitatively.

Table 2. Inferior to anterior wall ratio (Inf/Ant Ratio), septal to lateral wall ratio (Sept/Lat Ratio), and the average \pm standard deviation of the 17-segment perfusion scores for the NAC and AC images.

	Inf/Ant Ratio	Sept/Lat Ratio	17-Segment
NAC	0.99	1.17	78 \pm 6
AC	1.02	1.00	88 \pm 3

C. Defect Contrast

Fig. 6 displays the images of the cardiac insert with defects and the 17-segment perfusion map and scores. The calculated defect contrasts are shown in Table 3. The defect contrast is visually comparable for both of the full and 50% defect in the AC and NAC images. Quantitatively, AC images showed a significant defect contrast change over the NAC images for the full defect but only a marginal improvement for the 50% defect.

Table 3. Calculated defect contrast (DC) of the images of the cardiac insert with two defects.

	DC, Full Defect	DC, 50% Defect
NAC	0.528	0.156
AC	0.628	0.173

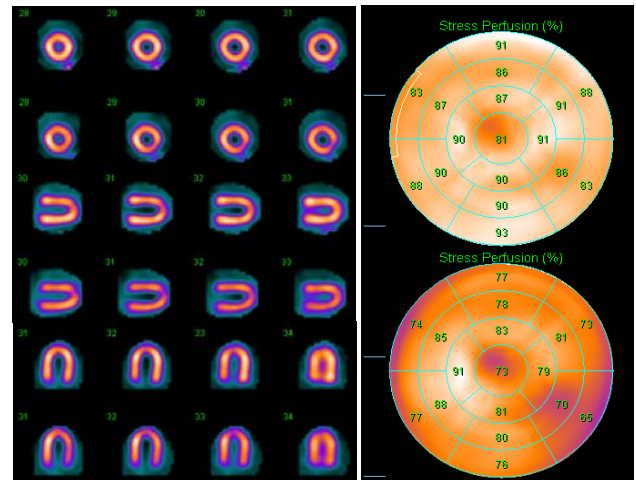


Fig. 5. Images and 17-segment perfusion scores of the uniform cardiac insert: First/top: AC, Second/bottom: NAC. AC significantly improved the uniformity as compared to NAC.

D. ACR Image Quality

Fig. 7 shows the reconstructed ACR phantom images with and without AC. AC corrected the bowing effect due to attenuation in the NAC image. AC images have balanced intensity in the transaxial slices but the NAC images are dimmer in the center than at the edge. The emission images of the uniform cylindrical phantoms also showed that AC corrected the bowing effect due to attenuation in the NAC images (images not shown).

IV. SUMMARY AND DISCUSSION

Phantom studies in this work showed that attenuation correction using the Cardius® X-ACT rapid SPECT/VCT imaging system was accurate and improved defect contrast. Over 300 patient studies have been presently performed at multiple centers (3) on the X-ACT system, results will be presented in a separate publication. With the high quality attenuation maps it generates and the low percentage of transmission/emission misregistration, X-ACT provides

a reliable and cost effective platform for the clinical incorporation of AC in routine practice to improve the effectiveness of patient care.

In the following sub-sections, we discuss some particular subjects of using the X-ACT for clinical applications.

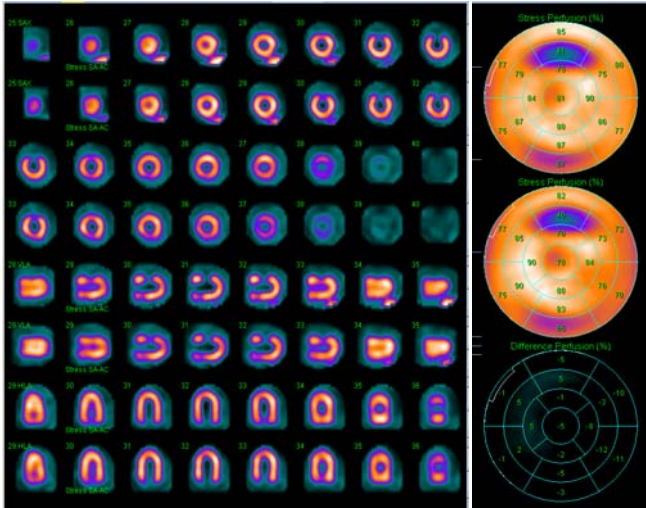


Fig. 6. Images and 17-segment perfusion polar maps and scores of the cardiac insert with two defects: First/top: AC, Second/bottom: NAC. AC improved the defect contrast.

A. Transmission/Emission Misregistration

Transmission/emission misregistration is a key factor that affects the accuracy of attenuation correction in SPECT. The system coregistration error due to system mechanics introduces the first level of emission/transmission misregistration. For example, when using a hybrid SPECT/CT system that uses sliding pallets to transport patient from SPECT to CT or vice versa, potential pallet sagging can introduce emission/transmission misregistration. Such misregistration usually increases with increased patient weight. For the X-ACT system, once the system is mechanically aligned, the transmission and emission coregistration errors for patient studies are minimal. This is due to the fact that (1) the fully integrated system eliminates the transportation of the patient between emission and transmission scans and (2) the patient chair is designed so that during the chair rotation, for patient up to 500 lbs (202.5 kg) the deflection of the chair and rotational inaccuracy is negligible.

Other than the system coregistration error, the major intrinsic source of misregistration is the patient respiratory motion. If the emission data and transmission data are acquired so that they include different respiratory motion patterns, misregistration will occur, no matter the transmission and emission scans are simultaneous or sequential. In cardiac SPECT, the emission scans take multiple minutes thus always

include many respiratory cycles. Our previous study [19] showed that a transmission scan including two or more respiratory cycles using the X-ACT system showed insignificant difference from a transmission scan that included many respiratory motions. This suggests the minimal time requirement for a transmission scan to minimize respiratory motion related misregistration. When using the hybrid SPECT/CT systems in which CT rotation speed is usually high, optimization of patient respiratory protocol may be needed to reduce the misregistration [24].

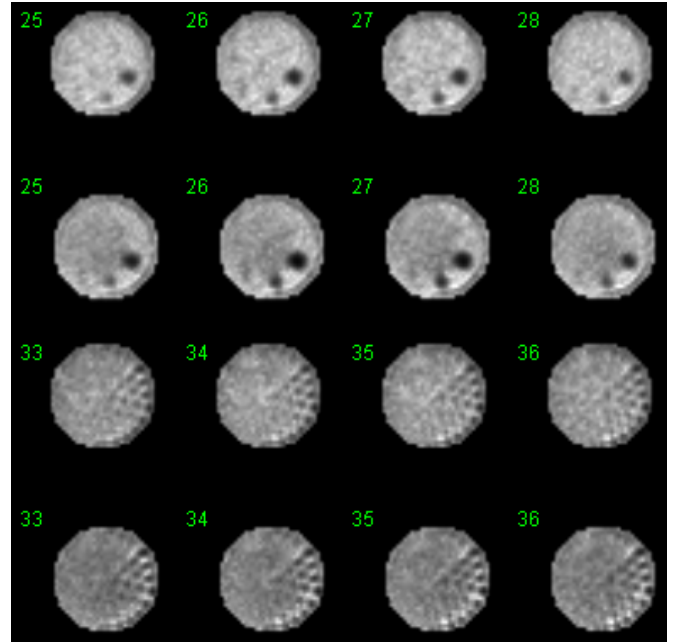


Fig. 7. Images of an ACR phantom with AC (top) and NAC (bottom). AC corrected the bowing effect due to attenuation shown in the NAC image. Note that the phantom has a diameter of 20 cm that is of the same size of the detector for emission scans. When fan-beam geometry is used, the emission image is slightly truncated (partial truncation rings shown in the images).

Another major source of transmission/emission misregistration is voluntary patient motion during sequential transmission and emission scans. Patient may have voluntary motion during the emission scan, or during the transmission scan, or during the transition from one scan to the other, or a combination of two or all of these motions. Misregistration caused by voluntary patient motion can be reduced through better patient preparation, and more efficient acquisition protocol that requires less acquisition time.

B. Transmission Source Strength and Scan Time

We mentioned in the Method section that the X-ACT transmission source has a flux rate of about 80 times that of the isotopic transmission sources used on commercial SPECT systems with isotopic AC. We noticed that X-ACT transmission photons (~ 77 keV)

have lower penetration power than Gd-153 transmission photons (~100 keV) due to the energy difference between the two. The effective flux rate advantage of the X-ACT transmission source over the Gd-153 transmission sources will decrease as the patient size increases. Starting from a ratio of 80, Table 4 illustrates the effective ratio of the transmission flux rate of the X-ACT transmission source to that of Gd-153 sources when passing through different thicknesses of water. The X-ACT transmission source is effectively 43 times as strong as Gd-153 source when passing through 40 cm of water, and 32 times as strong when passing through 60 cm of water.

The anthropomorphic phantom used in this work is a medium to large torso phantom with lateral dimension of 38 cm and anterior/posterior dimension of 26 cm. The effective transmission flux rate of the X-ACT transmission source for this phantom study is more than 43 times that of the Gd-153 sources. Therefore, a 1-minute transmission scan using the X-ACT system has over 14 times ($43/3 \approx 14$) the counts as a 3-minute scan using Gd-153 transmission sources. This explains the observed low noise level in the reconstructed attenuation maps. And similarly, for the same medium to large torso phantom, a 30-second transmission scan will result in over 7 times the counts of a 3-minute transmission scan using Gd-153 sources on current commercial systems, this suggests that one can do 30-second transmission scans using the X-ACT system and still obtain high quality transmission data, allowing 1-minute total transmission scan time that includes both the transmission acquisition and the emission contamination acquisition.

Table 4. Effective flux rate ratio of the X-ACT transmission source to that of Gd-153 transmission sources when passing through different thicknesses of water, starting with a ratio of 80 at 0 cm. The X-ray tube is operated at 160 kVp and 2.0 mA.

Water (cm)	0	10	20	30	40	50	60
Ratio	80	69	59	51	43	37	32

C. Patient Dose

When the X-ray tube operates at 160 kVp and 3.0 mA, the measured patient dose was 5.0 μ Sv for a one-minute transmission scan. For comparison, Table 5 lists the patient dose from conventional SPECT emission scans and the dose from transmission scans using isotopic sources or X-ray in hybrid SPECT/CT system. It is obvious that the transmission dose from X-ACT is negligible as compared to what one gets from the SPECT emission scan or the average background radiation in the US [25].

D. Room Shielding

The X-ACT system uses a low dose X-ray generator to produce attenuation maps for attenuation correction

of cardiac SPECT studies. Because an X-ray generator is used, medical facilities that use this system shall meet the shielding design goals specified in the National Council on Radiation Protection and Measurements (NCRP) Report No 147 [26] in order to limit the radiation exposure to the users and public members. This report is referred to as the Report hereafter.

Table 5. Dose for SPECT transmission imaging using X-ACT at 160 kVp and 3.0 mA and its comparison with the dose associated with some common circumstances.

	Patient Dose (mSv)	Times that of X-ACT Dose
SPECT transmission scan with Gd-153 sources	~ 0.002	0.4
X-ACT transmission scan	0.005	1.0
Chest X-ray	0.1	20
Low-Dose CT, non-diagnostic*	~0.9 to 2.0	180 to 400
Diagnostic CT**	6.0	1200
Cardiac SPECT, 99mTc-MIBI, Stress***	6.0	1200
Cardiac SPECT, Tl-201***	15.0	3000
Average US background radiation per year***	~ 3.6	720

* Such as GE Hawkeye, Philips BrightView

** Such as Philips Precedence, Siemens Symbia

*** From International Atomic Energy Agency [25]

According to the Report, the structural shielding shall keep the measured scatter air kerma within 0.1 mGy/week for controlled areas and primary air kerma within 0.02 mGy/week for uncontrolled areas. When a Cardius X-ACT system was installed in a room of 7 feet by 8 feet (2.13 m by 2.44 m) with two sheets of sheetrock in the walls, the measured scatter air kerma was 0.0016 mGy/week for controlled areas and the primary scatter air kerma was 0.0025 mGy/week for uncontrolled areas. The measurement was conducted when the X-ray tube was operated at the highest voltage and current combination for patient studies.

For both controlled and uncontrolled areas, the measured radiation level when using the Cardius X-ACT system is significantly lower than the limit stated in the Report. When considering wall shielding (for uncontrolled areas) particularly, two thickest commercially available sheetrock sheets (thickness: 5/8", density: 1.1 g/cc) can attenuate Cardius X-ACT transmission photons by a factor between 2 and 3. This means that, if the wall is without the sheetrock sheets in the above measurement, the maximal primary air kerma for uncontrolled areas will be 0.0075 mGy/week. Such a maximum is still less than half of the limit (0.02 mGy/week) for uncontrolled areas per the Report. Walls

with sheetrock sheets or wallboard will only make the radiation level lower than this maximum.

Based on this result, we can conclude that the Cardius X-ACT system can be operated in rooms of 7 feet by 8 feet (2.13 m by 2.44 m) or larger without special shielding (lead-lined or others). The radiation exposure to both users and public members is well within the safe level stated in the NCRP Report No 147. This is primarily due to the very low-dose of the X-ray generator and sufficient self-shielding of the transmission assembly of the system. Digirad corporation recommends the X-ACT system be operated in rooms of 8 feet by 8 feet (2.44 m by 2.44 m) or larger.

E. Cost of AC in Routine Clinical Practice

The cost of incorporating AC in routine clinical practice includes the cost of the AC system and the operational cost.

The X-ACT system uses the same solid-state detectors for both the emission and transmission scans, this is a substantial cost saving as compared to the hybrid SPECT/CT systems that requires a separate detector system for CT scans.

The low dose X-ray tube in the transmission source assembly is turned on when the transmission scan starts and turned off when the transmission scan ends. The current of the X-ray tube is very stable thus the generated transmission flux is very stable as well. For one system that we analyzed we did not see significant transmission flux change after operating for eleven months (after many phantom studies and more than 150 patient studies). As compared to systems using isotopic transmission sources that have to compensate for flux rate drop due to source decay and periodically replace the expensive sources, the X-ACT system holds an obvious advantage over the former by generating superior transmission images in a more stable and lower cost way.

Due to the upright imaging geometry, the X-ACT system can be operated in rooms of size as small as 8 feet by 8 feet (2.44 m by 2.44 m) and requires no special room shielding or use of an X-ray or CT technologist to operate the system as required by some states in the United States. In contrast, hybrid SPECT/CT systems in general require room sizes three to five times as large and special shielding of the room (except Philips BrightView XCT [27] that only requires minimal shielding), as well as the need for an X-ray or CT technologist or the Nuclear Medicine technologist with special certification the CT scans due to high dose required by some states in the US. The favorable differences of the X-ACT reflect a substantial cost reduction to care providers.

V. CONCLUSION

The transmission flux rate of the Cardius® X-ACT system is over 80 times that of conventional SPECT AC systems with isotopic transmission sources. The fully integrated SPECT/VCT design eliminates the need of patient translation between emission and transmission scans. The rapid imaging detector geometry enables high quality emission studies to be acquired in as little as three minutes or up to four times faster than conventional dual-head systems. High quality non-truncated transmission scans can be acquired in one minute without respiratory motion artifacts for attenuation correction as have been observed in in-line hybrid SPECT/CT systems. Phantom studies showed that the X-ACT system generated high quality and quantitatively accurate attenuation maps. Attenuation correction using the reconstructed attenuation maps in a 3D OSEM algorithm improved both image quality and quantification as desired.

VI. ACKNOWLEDGEMENT

We thank Rex Old for help with the manuscript. This work is fully supported by Digirad Corporation.

VII. REFERENCES

- [1] S. J. Cullom, *et al*, "Attenuation correction for cardiac SPECT: Clinical and developmental challenges," (invited commentary) *J. Nucl. Med.*, vol. 41, no. 5, pp. 860-862, 2000.
- [2] G. Germano, *et al*, "Attenuation correction in cardiac SPECT: The boy who cried wolf?" *J. Nucl. Cardiol.*, vol. 14, no. 1, pp. 25-35, 2007.
- [3] B. Singh, *et al*, "Attenuation artifact, attenuation correction, and the future of myocardial perfusion SPECT," (editorial point of view) *J. Nucl. Cardiol.*, vol. 14, no. 2, pp. 153-164, 2007.
- [4] P. B. Gibson, *et al*, "Low event rate for stress-only perfusion imaging in patients evaluated for chest pain," *J. Am. Coll. Cardiol.*, vol. 39, pp. 999-1004, 2002.
- [5] G. V. Heller, *et al*, "American Society of Nuclear Cardiology and Society of Nuclear Medicine joint position statement: Attenuation correction of myocardial perfusion SPECT scintigraphy," (joint position statement) *J. Nucl. Cardiol.*, vol. 11, no. 2, pp. 229-230, 2004.
- [6] D. D. Watson, "Is it time for SPECT attenuation correction?" *J. Nucl. Cardiol.*, vol. 11, no. 3, pp. 239-241, 2004.
- [7] J. Maddahi, *et al*, "Prospective multicenter evaluation of rapid, gated SPECT myocardial perfusion upright imaging," *J. Nucl. Cardiol.*, vol. 16, no. 3, pp. 351-357, 2009.
- [8] J. A. Patton and T. G. Turkington, "SPECT/CT physical principles and attenuation correction," *J. Nucl. Med. Technol.*, vol. 36, no. 1, pp. 1-10, 2008.

- [9] S. Goetze and R. L. Wahl, "Prevalence of misregistration between SPECT and CT for attenuation-corrected myocardial perfusion SPECT," *J. Nucl. Cardiol.*, vol. 14, no. 2, pp. 200-206, 2007.
- [10] C. Bai, *et al.*, "A Generalized Model for the Conversion from CT Numbers to Linear Attenuation Coefficients", *IEEE Trans. Nucl. Sci.* vol. 50, pp. 1510-1515, Oct 2003.
- [11] R. Conwell, *et al.*, "A novel cardiac SPECT system with X-ray-based attenuation correction using the same solid state detectors for both emission and transmission scans," *J. Nucl. Med.*, Vol. 49 (suppl.), 64p, 2008. Available at: http://jnumedmtg.snmjournals.org/cgi/content/meeting_abstract/49/MeetingAbstracts_1/64P-b.
- [12] H. Lewin and M. Hyun, "A clinical comparison of an upright triple-head digital detector system to a standard supine dual-head gamma camera," *J. Nucl. Cardiol.*, vol. 12, no. 4, Suppl. S, pp. S113-S113, 2005.
- [13] J. Chen, *et al.*, "Transmission scan truncation with small-field-of-view dedicated cardiac SPECT systems: Impact and automated quality control," *J. Nucl. Cardiol.*, vol. 12, pp. 567-573, Sep-Oct 2005.
- [14] J. Kindem, *et al.*, "Fluorescent X-ray line source generated by X-ray tube," US Patent (*pending*), 2008.
- [15] A. Celler, *et al.*, "Problems created in attenuation-corrected SPECT images by artifacts in attenuation maps: A simulation study," *J. Nucl. Med.*, vol. 46, no. 2, pp. 335-343, 2005.
- [16] http://xdb.lbl.gov/Section1/Table_1-3.pdf.
- [17] C. Bai, *et al.*, "A slice-by-slice blurring model for 3D scatter compensation in parallel and converging beam SPECT," *Phys. Med. Biol.*, vol. 40, pp. 1275-1307, 2000.
- [18] C. Bai and R. L. Conwell, "Emission-data-based photon scatter correction in computed nuclear imaging technology," US patent (*pending*), Document number: 20070200066, 2006.
- [19] R. Conwell, *et al.*, "Evaluation of the respiratory motion effect on transmission scans using an ultra-low dose X-ray-derived source," (Abstract), *J. Nucl. Med.*, vol. 50, 294P, May 2009.
- [20] R. Conwell, *et al.*, "Evaluation of image registration in a solid state cardiac SPECT system with an ultra-low dose X-ray-based attenuation correction," (Abstract, in press) *J. Nucl. Cardiol.*, 2009.
- [21] J. Maddahi, *et al.*, "Clinical evaluation of a low-dose, X-ray-based transmission imaging for attenuation correction of SPECT myocardial perfusion images," (Abstract), *J. Nucl. Med.*, vol. 50, 156P, May 2009.
- [22] K. J. Nichols, *et al.*, "Instrumentation quality assurance and performance," *J. Nucl. Cardiol.*, vol. 14, no. 6, pp. e61-e78, 2007.
- [23] Site Scanning Instructions for Use of the Nuclear Medicine Phantom for the ACR Nuclear Medicine Accreditation Program, American College of Cardiology.
- [24] D. Utsunomiya, *et al.*, "Object-specific attenuation correction at SPECT/CT in thorax: Optimization of respiratory protocol for image registration," *Radiol.*, vol. 237, no. 2, pp. 662-669, 2005.
- [25] Cardiac CT – radiation doses, dose management and practical issues, International Atomic Energy Agency, available at: http://rpop.iaea.org/RPOP/RPoP/Content/Documents/TrainingCardiology/Lectures/CARD_L11_CardiacCT_WEB.ppt
- [26] G. J. Chalmers, "Structural shielding design for medical X-ray imaging facilities (NCRP Report No 147)," *Phys. Med. Biol.*, vol. 50, pp. 4243-4244, 2005.
- [27] Philips BrightView XCT, company website, available at: <http://www.medical.philips.com/main/products/nuclearmedicine/products/brightviewxct/index.wpd>